AD-A183 639 RCCONSTRUCTION OF TOMOGRAPHIC IMAGES FROM SPARSE DATA 1/1
SETS BY A NEW FINIT..(U) ARMY BALLISTIC RESEARCH LAB
ABERDEEN PROVING GROUND MD R T SMITH ET AL. 07 APR 87
UNCLASSIFIED BRL-TR-2797 F/G 12/2 NL

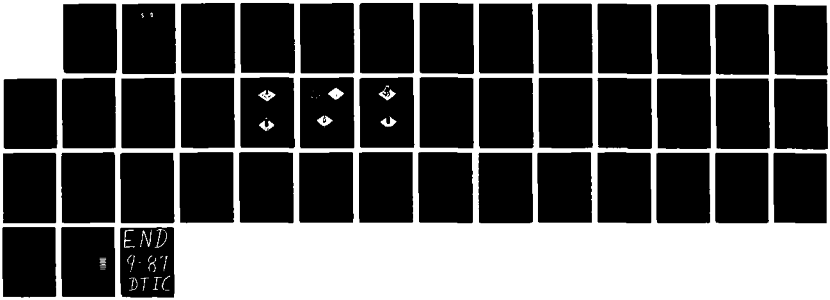

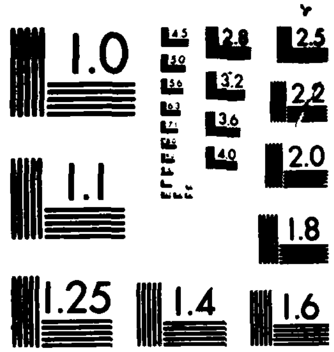

MICROCOPY RESOLUTION TEST CHART
NATIONAL BUREAU OF STANDARDS-1963-A

TECHNICAL REPORT BRL-TR-2797

RECONSTRUCTION OF TOMOGRAPHIC IMAGES FROM SPARSE DATA SETS BY A NEW FINITE ELEMENT MAXIMUM ENTROPY APPROACH

R. T. SMITH
C. K. ZOLTANI
G. J. KLEM

APRIL 7, 1987

US ARMY BALLISTIC RESEARCH LABORATORY
ABERDEEN PROVING GROUND, MARYLAND

UNCLASSIFIED

SECURITY CLASSIFICATION OF THIS PAGE

REPORT DOCUMENTATION PAGE

Form Approved
OMB No 0704-0188
Exp Date Jun 30, 1986

1a. REPORT SECURITY CLASSIFICATION Unclassified	1b. RESTRICTIVE MARKINGS
2a. SECURITY CLASSIFICATION AUTHORITY	3. DISTRIBUTION/AVAILABILITY OF REPORT
2b. DECLASSIFICATION/DOWNGRADING SCHEDULE	
4. PERFORMING ORGANIZATION REPORT NUMBER(S)	5. MONITORING ORGANIZATION REPORT NUMBER(S)
6a. NAME OF PERFORMING ORGANIZATION Ballistic Research Laboratory 6b. OFFICE SYMBOL (If applicable) SLCBR-IB-A	7a. NAME OF MONITORING ORGANIZATION
6c. ADDRESS (City, State, and ZIP Code) Aberdeen Proving Ground Maryland 21005-5066	7b. ADDRESS (City, State, and ZIP Code)
8a. NAME OF FUNDING/SPONSORING ORGANIZATION 8b. OFFICE SYMBOL (If applicable)	9. PROCUREMENT INSTRUMENT IDENTIFICATION NUMBER
8c. ADDRESS (City, State, and ZIP Code)	10. SOURCE OF FUNDING NUMBERS PROGRAM ELEMENT NO. 61102A PROJECT NO. 1L161102AH43 TASK NO 00 WORK UNIT ACCESSION NO

11. TITLE (Include Security Classification)
Reconstruction of tomographic Images from Sparse Data Sets by a New Finite Element Maximum Entropy Approach

12. PERSONAL AUTHOR(S)
R. T. Smith,* C. K. Zoltani, G. J. Klem

13a. TYPE OF REPORT	13b. TIME COVERED	14. DATE OF REPORT (Year, Month, Day)	15. PAGE COUNT
Technical Report	FROM 1984 TO 1986		

16. SUPPLEMENTARY NOTATION
*Virginia Polytechnic Institute, Blacksburg, VA 24061-4097

17. COSATI CODES			18. SUBJECT TERMS (Continue on reverse if necessary and identify by block number)
FIELD	GROUP	SUB-GROUP	Computed Tomography, Reconstruction, Image Analysis, Finite Element Method, Sparse Data Analysis, Image Reconstruction, Finite Element Method
19	01		
21	02		

19. ABSTRACT (Continue on reverse if necessary and identify by block number)

A new algorithm for the reconstruction of tomographic images from parse data sets is presented. A finite element technique was devised to solve the constrained optimization problem which resulted from the analysis using the maximum entroy formalism. the improvement in reconstruction image quality over conventional techniques is illustrated by several examples.

20. DISTRIBUTION/AVAILABILITY OF ABSTRACT ☒ UNCLASSIFIED/UNLIMITED ☒ SAME AS RPT ☒ DTIC USERS	21. ABSTRACT SECURITY CLASSIFICATION Unclassified
22a. NAME OF RESPONSIBLE INDIVIDUAL Csaba K. Zoltani	22b. TELEPHONE (Include Area Code) (301) 278-6108 22c. OFFICE SYMBOL SLCBR-IB-A

DD FORM 1473, 84 MAR

83 APR edition may be used until exhausted
All other editions are obsolete

SECURITY CLASSIFICATION OF THIS PAGE
UNCLASSIFIED

TABLE OF CONTENTS

LIST OF ILLUSTRATIONS

I. INTRODUCTION

The quality of tomographic images reconstructed from sparse data sets usually suffers from the presence of artifacts, fuzziness and a loss of resolution. Sparse data problems arise typically in situations where only a few views are available, where there is an angular restriction in taking the data, or where the object of interest is partly obstructed.

Previous attempts at sparse data reconstructions[1] have met with varying degrees of success. Here we present a new algorithm based on the maximum entropy formalism[2] and formulated as a constrained optimization problem which is solved by a finite element method. The results show encouraging improvement over conventional sparse data reconstructions. In particular, the MENT algorithm of Minerbo[2] requires that the input density data "falls-off" to zero towards the edges of the target grid. The present method has no such restriction on the input data. Of course, in practice, the MENT restriction means that the x-ray sources and detector arrays must be pulled back, away from the object of interest, so that the object is surrounded by some medium of known density. This known background density may then be subtracted from the actual measured data, resulting in modified data indicating zero density near the edges. Naturally, there is a physical restriction resulting from this mathematical "edge condition". That is, given a fixed scanning installation, the MENT algorithm may only be used to reconstruct density profiles of objects whose size is somewhat smaller than that which the machinery itself would otherwise permit. This restriction becomes particularly severe, then, in the case of industrial tomography, where the objects of interest are already rather large.

Computational experience at this laboratory and elsewhere has demonstrated that in cases where data is sparse, i.e. where fewer than 180 views are available or where the number of detectors per view are less than 100, filtered backprojection, the algorithm of choice for modern CAT scanners, produces an image inferior in quality to that obtainable from maximum entropy. The explanation seems to revolve around the built-in smoothing of the entropy approach which was developed on ideas based on Shannon's information theory.

In this study the maximum entropy method is reformulated and coupled with a finite element approach. This new algorithm is described in the second chapter followed by several examples. An example of an object with nonzero density near the edge of the target grid has been included. We demonstrate both the MENT reconstruction of this image (which is thoroughly unrecognizable) and the reconstruction by our new algorithm, using the same measured input data The concluding chapter discusses the results. The Appendix lists the computer program which was developed for this work.

---

[1] A.K. Louis, "Approximation of the Radon Transform from Samples in Limited Range." in Lecture Notes in Medical Informatics, Vol. 8, pp.127-139, 1981.

[2] G. Minerbo, "A Maximum Entropy Algorithm for Reconstructing a Source from Projection Data." Comp. Graph. Image Proc. Vol. 10, pp.48-68, 1979.

II. THE ALGORITHM

A. Background

Computed tomography enables the determination of density cross-sections of slices of an object in the plane of a radiation source from the recorded absorption levels of the transmitted radiation. From the early work of Radon[3] we know that the problem can be formulated mathematically as an inverse problem and a unique solution, i.e. a reconstructed image is guaranteed when data from an infinite number of views is available. If only a finite number of views are available, mathematically the problem becomes ill posed and small changes, i.e. discrepancies, are amplified leading to inaccurate image representation.

Techniques have been developed, however, to overcome this problem and to obtain excellent images. Of course, image quality also improves with an increase in the number of views. In this study we look at the case of 21 views with at least 50 detectors per view. The problem of well posedness, existence, uniqueness of our formulation are dealt with in an accompanying report[4]. Here we present a new algorithm for the reconstruction of the image which for sparse data sets yields fewer artifacts than conventional approaches.

B. General Formulation

Central to the idea of tomographic reconstruction, given a radiation source, a detection system and an object placed in the path of the radiation, (see Fig. 1a) is the fact that data is obtained as a set of integrals. Thus, let $f(x,y)$ be the x-ray attenuation at a point (x,y) in the plane. Measured data, G_{jm}, is available in the form

$$G_{jm} = S_{jm}(f) = \int_{S_{jm}}^{S_{jm+1}} \int_{-\infty}^{+\infty} f(s \cos \theta_j - t \sin \theta_j,\ s \sin \theta_j + t \cos \theta_j)\, dt\, ds$$

$$m = 1, \ldots m(j);\quad j = 1, \ldots J, \qquad (1)$$

where J is the number of projections and $m(j)$ the number of detectors for the j-th view and θ is the scan angle.

The object of interest lies in a finite region $\mathcal{D}$ contained in $\mathbb{R}^2$. The entropy of the image can be defined as

[3] J. Radon, "Ueber die Bestimmung von Funktionen durch ihre Integralwerte laengs gewisser Mannigfaltigkeiten." Ber. Verh. Saechs. Akad. Wiss. Leipzig, Math. Phys. Kl. Vol. 69, pp. 262-277, 1917.

[4] R.T. Smith, C.K. Zoltani, "An Application of the Finite Element Method to Maximum Entropy Tomographic Image Reconstruction." BRL Report (in preparation).

$$\eta(f) = -\int\int_{\mathfrak{D}} \left|f(x,y)\right| \ln\left[\left|f(x,y)\right| A\right] dxdy \qquad (2)$$

where A is the area of $\mathfrak{D}$ and $f \varepsilon \mathcal{L}^2(\mathfrak{D})$, the set of square integrable functions in $\mathfrak{D}$, i.e.

$$\int\int_{\mathfrak{D}} f^2 \, dA < \infty \text{ holds.} \qquad (3)$$

Deviating from previous approaches, instead of maximizing the entropy with the measured values as constraints, we minimize minus the entropy plus a penalty term subject to some known, a priori bounds. That is, f can be determined as the solution of the constrained optimization problem

$$\inf_{f \in \Sigma} E(f) = \inf_{f \varepsilon \Sigma} -\eta(f) + \gamma \sum_{j,m} (G_{jm} - S_{jm}(f))^2 \qquad (4)$$

where the constraints set Σ is defined as

$$\Sigma = \{ f \varepsilon \mathcal{L}^2(\mathfrak{D}): a \le f \le b, \text{ and } f = 0 \text{ in } \mathbb{R}^2 \setminus \mathfrak{D}\} \qquad (5)$$

where we usually require $a > 0$ and $b < \infty$.

From the theory of penalty functions, we know that if we take $\Sigma = \mathcal{L}^2(\mathfrak{D})$, then as $\gamma \to \infty$, the solution of the unconstrained minimization problem converges to the solution of the equality constrained problem solved by Minerbo[2]. By taking a sufficiently large value of the penalty parameter γ, the residual error, $\sum (G_{jm} - S_{jm}(f))^2$ can be made sufficiently small to achieve the desired fidelity in the reconstructed image. In practice, of course, the values of G_{jm} are degraded by noise and we wish only to obtain a total residual error within some tolerance determined by the known accuracy of the measurements. Also, we have included a priori information in the problem formulation, by choosing a and b so that the attenuation lies within some known physical limits.

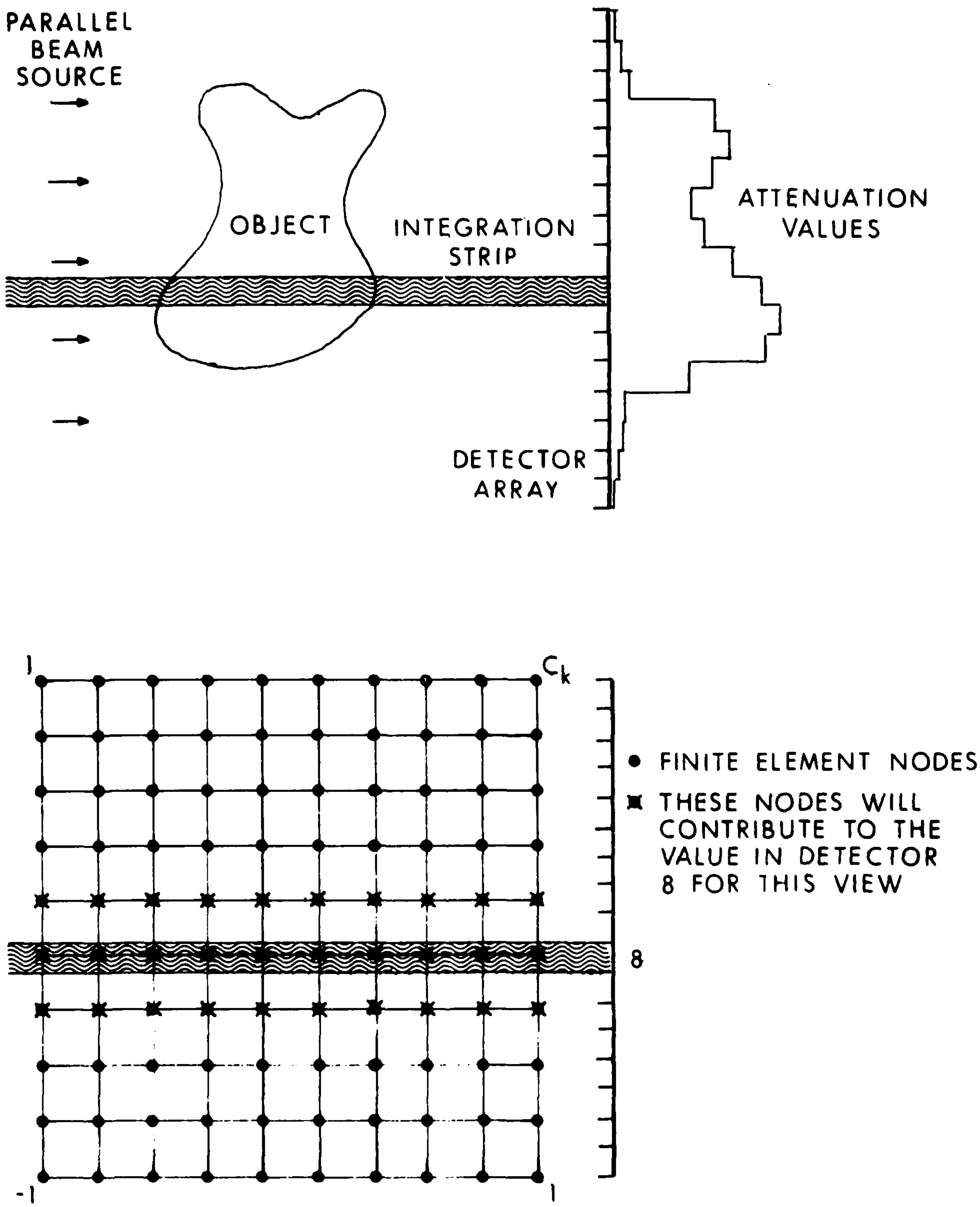

Figure 1. Scanning Geometry

The solution of (4) can be approximated by solving the problem in a finite dimensional subspace of $\ell^2(\mathscr{D})$, S^h. Let $\{\phi_1(x),\ldots,\phi_n(x)\}$ be a basis for S^h and for any $c = (c_1,c_2,\ldots,c_n)$ in $\mathbb{R}^n$ let

$$f_c(x) = \sum_{i=1}^{n} c_i\phi_i(x). \tag{6}$$

It is shown in [4] that, for a certain class of approximating subspaces (including the one used in the present work), the solution of (4) out of S^h converges to the solution of the infinite dimensional optimization problem, as h tends to zero. Precise estimates of the deviation of the reconstructed image from that of the true phantom are out of the question at this time, as an analytic relationship between the maximum entropy solution and the true image is unknown.

The finite dimensional constrained optimization problem then, is to determine f_c which minimizes

$$E(f_c) = -\eta\Big(\sum_i c_i\phi_i\Big) + \gamma\sum_{j,m}\Big(G_{jm} - S_{jm}\Big(\sum_i c_i\phi_i\Big)\Big)^2 \tag{7}$$

subject to

$$a \le \sum_i c_i\phi_i(x) \le b, \text{ for all } x \in \mathscr{D} \text{ and } a > 0.$$

To solve this nonlinear, convex programming problem, a uniform mesh is superimposed on the region $\mathscr{D}$ with step size h in both coordinate directions. A product of piecewise linear functions, $\phi_{ij}(x,y)$,

$$\phi_{ij}(x,y) = \phi_i(x)\phi_j(y), \qquad \begin{array}{l} i = 1,\ldots m_1 \\ j = 1,\ldots m_2 \end{array} \tag{8}$$

is used as a basis for S^h. Here, ϕ_i denotes the usual linear finite element basis function

$$\phi_i(x) = \begin{cases} 0, & \text{if } x \le x_{i-1} \text{ or } x \ge x_{i+1} \\ (x - x_{i-1})/h & \text{if } x_{i-1} \le x \le x_i \\ (x_{i+1} - x)/h & \text{if } x_i \le x \le x_{i+1} \end{cases} \tag{9}$$

where $x_i = ih$.

For convenience, we write

$$\phi_k(x,y) = \phi_i(x)\phi_j(y), \quad k = i + (j-1)m_1 \qquad (10)$$

then

$$f_c(x,y) = \sum_{k=1}^{M} c_k \phi_k(x,y)$$

where $M = m_1 m_2$.

Noting the compact support of the ϕ_k's, it can be shown that

$$a \le f_c(x,y) \le b \text{ for all } (x,y) \in \mathcal{D}$$

if and only if $a \le c_k \le b$, for all $k = 1,\ldots M$.

The optimization problem reduces to one with linear inequality constraints, i.e. determine c which minimizes

$$E(f_c) = -\eta(f_c) + \gamma \sum_{j,m} (G_{jm} - S_{jm}(f_c))^2 \qquad (11)$$

subject to $\qquad a \le c_k \le b, \; k = 1,\ldots M.$

The problem then is to calculate the vector $c = (c_1,\ldots c_M)^T$ for given values of γ, a and b.

For the optimization step of the algorithm we used MINOS[5], a FORTRAN code developed for constrained optimization problems. The user supplies the function to be optimized, the constraints and some ancillary files.

The calculation proceeds as follows: a preprocessor program (see Fig. 2a) reads the number of nodes in the mesh geometry, the number of projection angles

[5]B.A. Murtagh, M.A. Saunders, "MINOS 5.0 User's Guide." Systems Optimization Laboratory, Department of Operations Research, Technical Report SOL 83-20, Stanford University, Stanford, CA, December, 1983.

and their values (the ANG.DAT file), and the number of detectors for each projection angle (view). The preprocessor creates a weights file SJM.DAT, which indicates the contribution of each particular finite element (geometry cell) to each detector at each angle.

The main program is the optimizing routine MINOS (see Fig. 2b). A first guess at the coefficients c_k is read into MINOS. On the first pass through, the subroutine FUNOBJ reads the measurements file GJM.DAT, which contains the attenuation values indicating how much of the incident beam was absorbed by its traverse through the target. These measurements values are scaled such that the maximum attenuation is set to 1.0. On each successive iteration, FUNOBJ accesses the weights file SJM.DAT in its calculation of the entropy ENT for the present values of the coefficients c_k and the terms

$$EN(k) = \int\int_{\mathcal{D}} \phi_k(x,y) \ \ln[\sum_{k=1}^{M} c_k\phi_k(x,y)] \ dxdy \qquad (12)$$

which are used in computing the gradient of the object function. For the quadrature of the equation (12) the adaptive grid routine QUANC8[6] was used.

With the value of ENT and EN(k), FUNOBJ will compute the values of the object function F(c) and the gradient function G where

$$F(c) = -\eta(\sum_{k=1}^{M} c_k\phi_k(x,y)) + \gamma\sum_{j,m} [G_{jm} - \sum_{k=1}^{M} c_k S_{jm}(\phi_k)]^2 \qquad (13)$$

and

$$G(c) = \nabla F(c) = \sum_{k=1}^{M} e_k(h^2 + \int\int_{E^k} \phi_k(x,y) \ \ln[\sum_{k=1}^{M} c_k\phi_k(x,y)] \ dxdy$$

$$- 2\gamma\sum_{j,m} [G_{jm} - \sum_{k=1}^{M} c_k S_{jm}(\phi_k)]S_{jm}(\phi_k) \qquad (14)$$

[6]G.E. Forsythe, M.A. Malcolm, C.B. Moler, Computer Methods for Mathematical Computations, Prentice Hall, 1977.

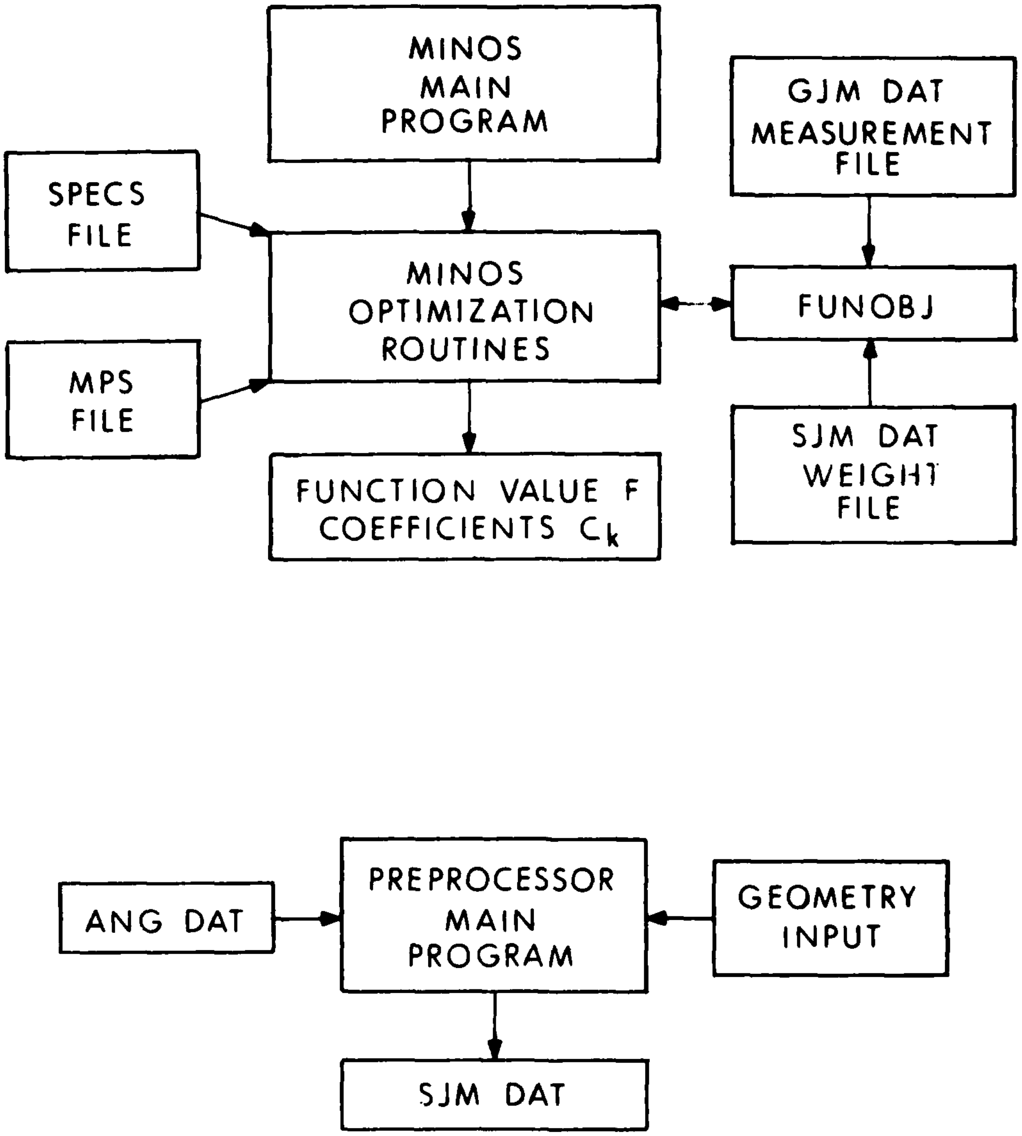

Figure 2. Flow Chart of the Algorithm

where e_k is the k-th unit vector, i.e. $e_k = (0,0,\ldots 1,\ldots 0)^T$ and E^k is the support of the k-th basis function, $\phi_k(x,y)$. The values of F and G are then passed back to MINOS for the next step in the optimization. The value of the penalty parameter γ is problem dependent and some experimentation is needed to determine the best value.[7]

The solution can be made arbitrarily close to the optimal solution by choosing a large enough value for γ. An analytical method for determining the optimal penalty is not available. Also, some caution needs to be exercised in picking the value to avoid ill-conditioning or slow convergence. In this problem the penalty parameter was increased gradually and it was found that $\gamma = 75$ yielded the best result, i.e. the smallest error in the reconstruction.

III. IMPLEMENTATION OF THE TECHNIQUE

A. Mathematical Phantoms

The computer code GOLEM[8] was used to generate the x-ray absorption data from mathematical phantoms for input to the reconstruction algorithms. For this study, three examples were generated, assuming a parallel mode of scanning, using a technique described in Ref. 8. Physically, the target objects are placed between a source of monochromatic parallel beam x-rays and a straight line of detectors perpendicular to the x-ray transmission. For each of the examples, the phantoms were set within a square target grid of 30 unit cells on each side. The x-ray source was placed 69 units from the center of the target grid. A line of 25 detectors was placed 16 units from the center of the target grid, opposite the x-ray source. Data was produced from five projection angles equally spaced around the target. A square reconstruction grid of 30 unit cells on each side spans the width of the 25 detector bins.

The first phantom consisted of a tube 6 units in diameter, with unit density on a 0.1 density background, whose center was placed on the axis of the field of scan. For the second sample problem, three identical, solid cylinders were placed at arbitrary positions within the target area. In the third problem, a solid cylinder was placed inside a thick-walled hollow cylinder, with both cylinders centered at the target origin. For all the examples, the cylinders were given a density of 1 while the remainder of the target grid was assigned a background density of 0.1. A cross-sectional view of the sample problems is given in Figure 1.

---

[7] M.S. Bazaraa, C.M. Shetty, Nonlinear Programming, John Wiley, New York, 1979.

[8] M.D. Altschuler, T. Chang, A. Chu, "Rapid Computer Generation of Three Dimensional Phantoms and Their Cone Beam X-Ray Projections." Medical Image Processing Group Technical Report No. MIPG 16, State University of New York at Buffalo, November 1978.

B. Results

The sample phantoms were reconstructed using our new algorithm and then compared with the results of the currently preferred sparse data technique MENT[2]. Figure 4a shows the reconstructed density plot of the first example using the new technique, while the adjoining Figure 4b illustrates the MENT results for the same problem. These figures are both three-dimensional grid representations of the reconstructed density (with hidden lines removed). The 31x31 grid used for the reconstruction (the actual finite element grid for Figure 4a) is shown in the middle of the 51x51 grid, with points outside the 31x31 grid being given density zero. One should note the high degree of correspondence between the reconstructions of Figures 4a and 4b.

Figure 5a gives the reconstructed density plot of the second example. The three solid cylinders of unit density stand out vividly against an undulating background of density 0.1. The five projection angles can be picked out as the "ridges" or "humps" which stretch through the object space in Figure 5a. One should notice from Figure 3b that one of the three cylinders is rather close to the edge of the target grid. The MENT algorithm has difficulty with nonzero density near edges. In Figure 5b one can see the MENT reconstruction of the second sample problem using the same projection data as that used in Figure 5a. Of course, the reconstruction is completely unrecognizable. In Figure 5c we demonstrate the results of a MENT run in which the data from the three cylinder geometry case is reconstructed in a larger area (a 51 x 51 grid). Moving the cylinders away from the edge of the reconstruction grid allows the MENT code to smooth its results to zero at the boundaries of the reconstruction grid. In particular, the MENT algorithm artificially forces the density to zero near the edges of the target grid, while the new method correctly shows a nonzero density.

The results for the third sample problem are given in Figures 6 and 7. Figure 6 gives density surface plots, comparing the new algorithm with MENT. Finally in Figure 7, a vertical slice through the center of the density plot is shown for both methods. In this case, note that there is very good agreement between the two methods. However, as with the second example, MENT has forced the density to zero near the edges.

The new algorithm was run on the CRAY XMP/12 computer at the Naval Research Laboratory in Washington, DC. The results shown were obtained using approximately 100 iterations of the MINOS optimization code and required approximately 10 minutes of cpu time. The MENT algorithm was run on the CDC CYBER 70/76 computer at the Ballistic Research Laboratory, Aberdeen Proving Ground, MD. These results required only a few seconds of cpu time.

Although the new method requires substantially more computer time and memory than the MENT algorithm, we believe that it still represents a significant advance. Very sparse data is all that is available in many industrial applications. One can employ no mathematical trickery to change this fact. In some of these cases, where the data fails to fall off to zero near the edges, the currently preferred method MENT will not produce an even remotely recognizable reconstruction. Our new algorithm has removed this "edge condition" restriction and although a costly process (in terms of computer time), it will yield a reasonable reconstruction. We believe that the computer

time and memory requirements may be reduced by developing more efficient codes for the computation of the cost functional and gradient terms in (13) and (14) and possibly by the development of a customized optimization routine.

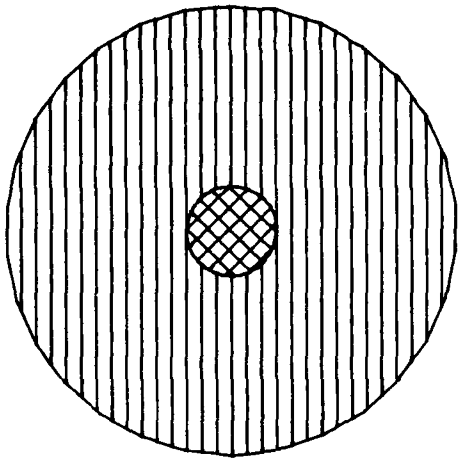

a. Sample Problem One.

	xc	yc	rad	density
background	0.0	0.0	15.0	0.1
1	0.0	0.0	3.0	1.0

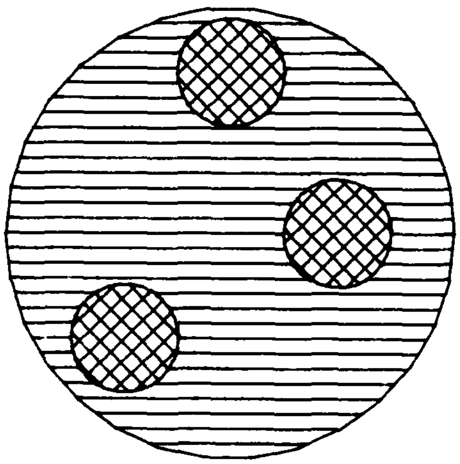

b. Sample Problem Two

	xc	yc	rad	density
background	0.0	0.0	15.0	0.1
1	-7.0	-7.0	3.6	1.0
2	0.0	10.7	3.6	1.0
3	7.2	0.0	3.6	1.0

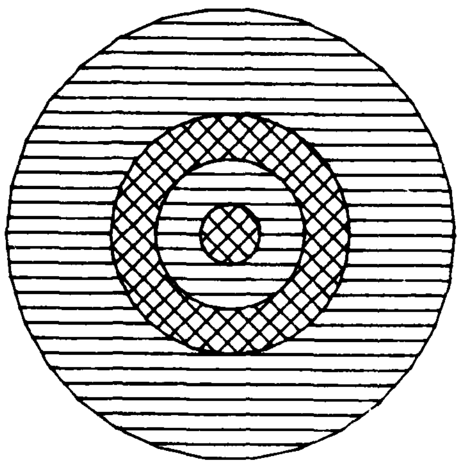

c. Sample Problem Three

	xc	yc	rad	density
background	0.0	0.0	15.0	0.1
1	0.0	0.0	2.0	1.0
2	0.0	0.0	5-8.0	1.0

Figure 3.a. Object Geometry Sample Problem One
b. Object Geometry Sample Problem Two
c. Object Geometry Sample Problem Three

a.

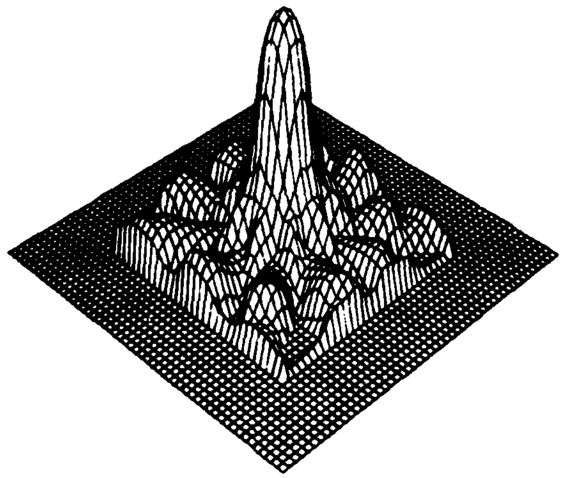

b.

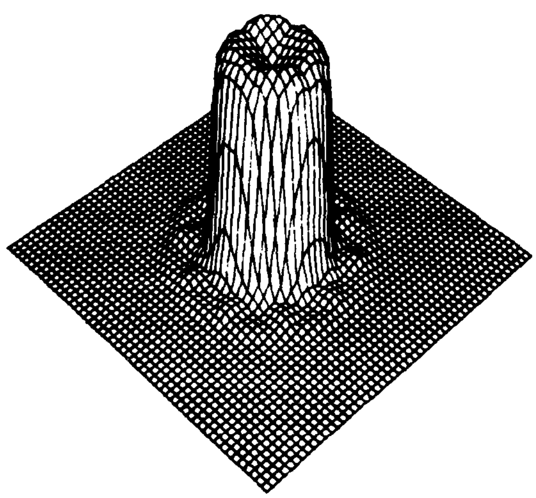

Figure 4. a. Sample Problem One: 3D Density Plot using FEME Code
b. MENT Results from the Same Data

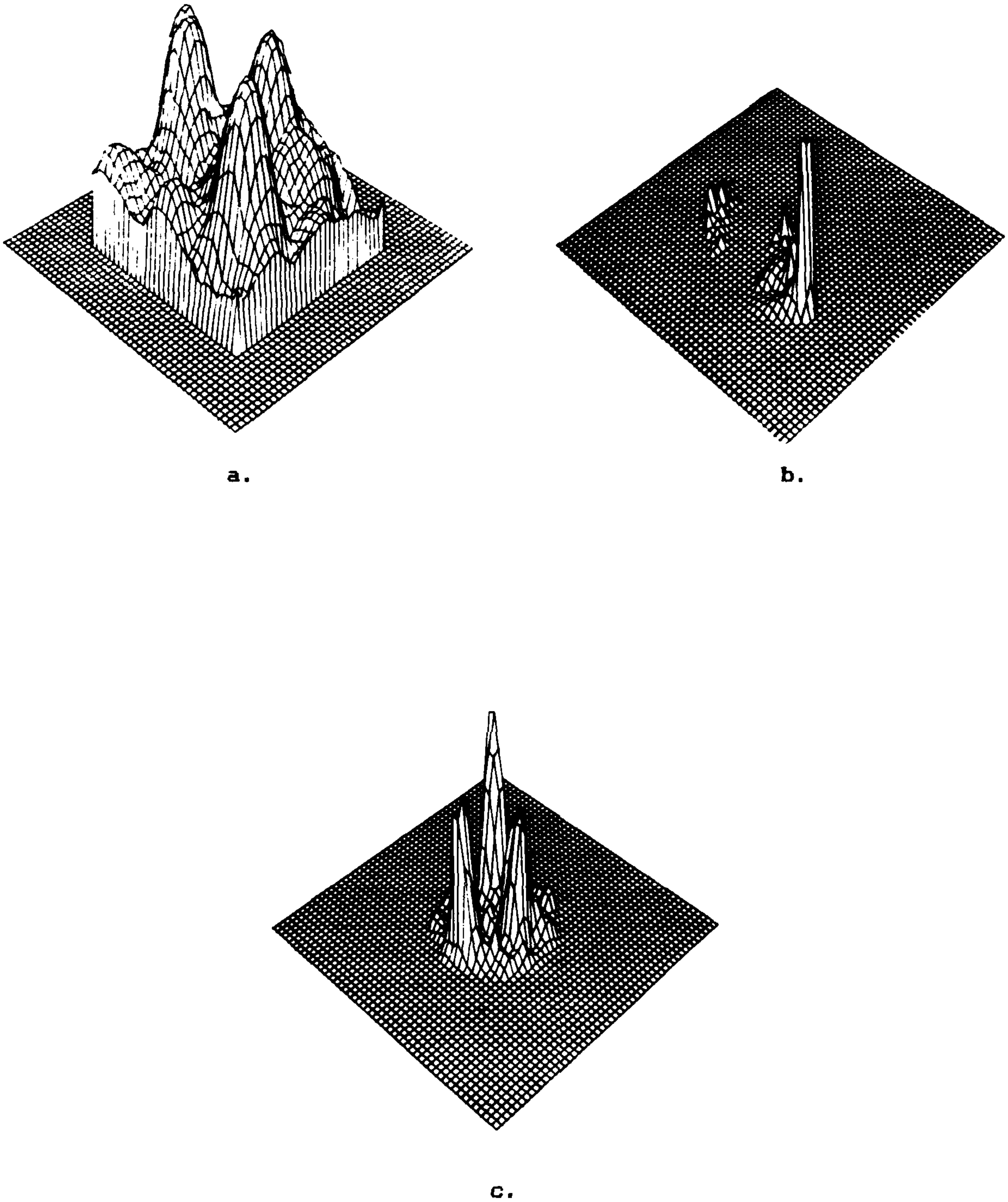

Figure 5. a. Sample Problem Number Two: 3D Density Plot Using FEME Code
b. MENT Results
c. MENT Results with Edge of Object Displaced from Edge of Computational Grid

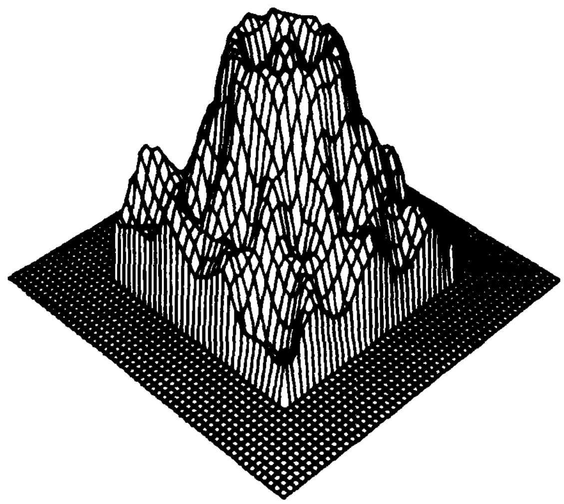

a.

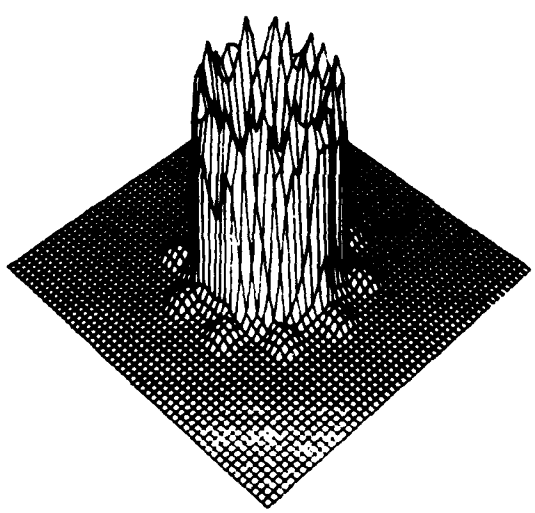

b.

Figure 6.a. Density Surface Plot, Problem Three: FEME Results
b. Density Surface Plot, Problem Three: MENT Results

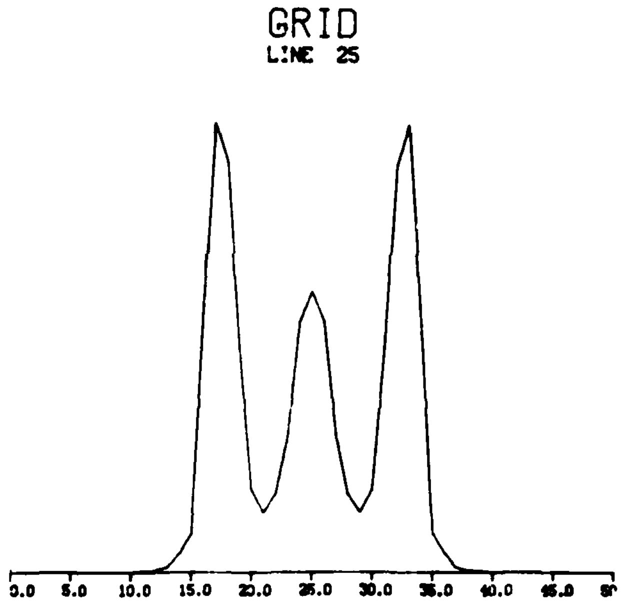

a.

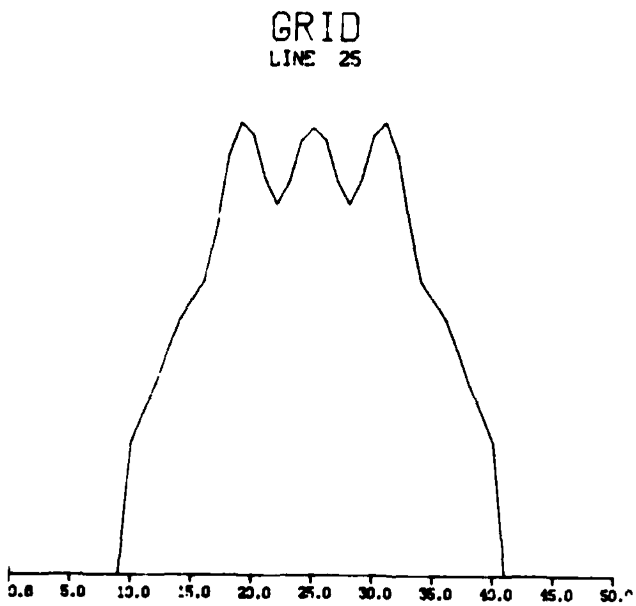

b.

Figure 7. a. Sample Problem Number Two: Center Slice, FEME Results
b. Sample Problem Number Two: Center Slice, MENT Results

ACKNOWLEDGEMENT

It is a pleasure to thank Mr. Monte Coleman not only for furnishing parallel beam scan data and the results of the MENT code, but also for his guidance in producing the graphical output for this report.

REFERENCES

1. A.K. Louis, "Approximation of the Radon Transform from Samples in Limited Range." in Lecture Notes in Medical Informatics, Vol. 8, pp.127-139, 1981.

2. G. Minerbo, "A Maximum Entropy Algorithm for Reconstructing a Source from Projection Data." Comp. Graph. Image Proc. Vol. 10, pp.48-68, 1979.

3. J. Radon, "Ueber die Bestimmung von Funktionen durch ihre Integralwerte laengs gewisser Mannigfaltigkeiten." Ber. Verh. Saechs. Akad. Wiss. Leipzig, Math. Phys. Kl. Vol. 69, pp. 262-277, 1917.

4. R.T. Smith, C.K. Zoltani, "An Application of the Finite Element Method to Maximum Entropy Tomographic Image Reconstruction." BRL Report (in preparation).

5. B.A. Murtagh, M.A. Saunders, "MINOS 5.0 User's Guide." Systems Optimization Laboratory, Department of Operations Research, Technical Report SOL 83-20, Stanford University, Stanford, CA, December 1983.

6. G.E. Forsythe, M.A. Malcolm, C.B. Moler, Computer Methods for Mathematical Computations, Prentice Hall, 1977.

7. M.S. Bazaraa, C.M. Shetty, Nonlinear Programming, John Wiley, New York, 1979.

8. M.D. Altschuler, T. Chang, A. Chu, "Rapid Computer Generation of Three Dimensional Phantoms and Their Cone Beam X-Ray Projections." Medical Image Processing Group Technical Report No. MIPG 16, State University of New York at Buffalo, November 1978.

APPENDIX

A listing of the computer code follows. Note that the MINOS subroutines are not included.

```
      SUBROUTINE FUNOBJ(MODE,NN,C,F,G,NSTATE,NPROB,Z,NWCORE)
C
C      THIS SUBPROGRAM WILL COMPUTE THE OBJECT FUNCTION (F)
C      AND ITS GRADIENT (G(K)) CORRESPONDING TO THE CURRENT
C      VALUES OF THE COEFFICIENTS, C(K) COMPUTED BY MINOS.
C
C      THESE VALUES ARE THEN PASSED BACK TO MINOS TO
C      CONTINUE THE OPTIMIZATION PROCESS.
C
C
      DIMENSION C(NN),EN(289),G(NN),GJM(231), SJMDAT(20000)
      LOGICAL FIRST
      DATA FIRST/.TRUE./
      WRITE(6,37)
   37 FORMAT(' THE COEFFICIENTS C(K)')
      WRITE(6,35) (C(INDEX),INDEX=1,289)
   35 FORMAT(17F7.3)
      IF (FIRST) THEN
         WRITE(6,22)
   22    FORMAT(' PERFORMING SET-UP OPERATIONS IN FUNOBJ')
         OPEN (4,FILE='SJMDAT',ACCESS='SEQUENTIAL',FORM='UNFORMATTED')
         READ (4) SJMDAT
         OPEN (7,FILE='GJMDAT')
         REWIND(7)
C
         N=8
         M=11
         JA=5
         IND=(2*N+1)**2
         H=1./N
C
C        N   = NUMBER OF GRID POINTS ON EITHER SIDE OF THE ORIGIN
C        M   = NUMBER OF PROJECTION STRIPS
C        JA  = THE NUMBER OF PROJECTION ANGLES, I.E. # OF VIEWS
C        IND = NUMBER OF FINITE ELEMENTS
C        H   = MESH WIDTH
C
C        THE GJM(N)'S ARE THE MEASUREMENTS OF THE X-RAY INTENSITY.
C        THESE ARE STORED IN THE FILE GJM.DAT.
C
         DO 492 JJA=1,JA
         DO 492 MA=1,M
  492      READ(7,493) GJM((JJA-1)*M+MA)
  493    FORMAT(E15.3)
         CLOSE(7,STATUS='DELETE')
         WRITE(6,38)
   38    FORMAT(' THE MEASUREMENTS FILE')
         DO 33 MA=1,M
   33      WRITE(6,495)(GJM((JJA-1)*M+MA),JJA=1,JA)
  495    FORMAT(1P5E15.3)
```

```
C        RELERR AND ABSERR ARE THE RELATIVE AND ABSOLUTE
C        ERRORS ALLOWED IN THE NUMERICAL INTEGRATIONS
C
         RELERR=5E-6
         ABSERR=0.
C
C        GAMMA IS THE PENALTY PARAMETER.
C        FOR CONVERGENCE TO THE MAXIMUM ENTROPY SOLUTION,
C        WE NEED TO TAKE A SEQUENCE OF VALUES OF GAMMA
C        TENDING TO INFINITY, OR TAKE A SUFFICIENTLY LARGE VALUE
C        OF GAMMA SO THAT THE RESIDUAL, RES IS SUFFICIENTLY SMALL.
C
         GAMMA=50.0
         WRITE(6,39) GAMMA
   39    FORMAT(' GAMMA=',F5.1)
         FIRST=.FALSE.
         WRITE(6,24)
  24     FORMAT(' FINISHED WITH SET-UP PROCEDURES IN FUNOBJ')
      ENDIF
C
      CALL ENTR(EN,ENT,N,RELERR,ABSERR,C)
C
C       THE SUBROUTINE ENTR COMPUTES THE VALUES OF THE ENTROPY
C       TERMS EN(K) AND THE ENTROPY ENT FOR THE CURRENT VALUES OF C(K)
C
      RES=0.
      DO 420 JTA=1,JA
         DO 420 MI=1,M
            SUM=0.
         DO 410 K=1,IND
            JJ = (K-1)*M+(JTA-1)*IND*M+MI
  32        FORMAT(' JJ=',I10)
C
C       MAINF.FOR COMPUTES THE VALUES OF SJM(K), BUT STORES THESE
C       VALUES IN SJM.DAT IN A DIFFERENT ORDER FROM THAT IN WHICH
C       THEY MUST BE ACCESSED BY FUN. JJ GIVES THE DESIRED RECORD
C       NUMBER IN THE DIRECT ACCESS FILE SJM.DAT.
C
410      SUM=SUM+C(K)*SJMDAT(JJ)
420      RES=RES+(GJM((JTA-1)*M+MI)-SUM)**2
C
C       RES IS THE RESIDUAL ERROR IN MEETING THE MEASUREMENTS.
C
      F = -ENT + GAMMA*RES
      WRITE(6,34) F,ENT,RES
   34 FORMAT(' F=',E14.5,' ENT=',E14.5,' RES=',E14.5)
```

```
C       THIS SECTION COMPUTES THE GRADIENT TERMS
C
      DO 440 K=1,IND
         SU2=0.
         DO 460 JTA=1,JA
            DO 460 MI=1,M
               SUM=0.
               DO 450 KI=1,IND
                  JJ=(KI-1)*M+(JTA-1)*IND*M+MI
 450              SUM=SUM+C(KI)*SJMDAT(JJ)
               J2=(K-1)*M+(JTA-1)*IND*M+MI
 460         SU2=SU2+(GJM((JTA-1)*M+MI)-SUM)*SJMDAT(J2)
 440      G(K) =-H*H*(1.+ALOG(4.)) + EN(K)-2.*GAMMA*SU2
               RETURN
C
  800 PRINT *, ' ERROR/FUNOBJ - EOF ON UNIT 4'
         STOP
  810 PRINT *, ' ERROR/FUNOBJ - ERR ON UNIT 4'
      PRINT *, '                         IOSTAT = ', IONUM
         STOP
      END
C
C
C
      SUBROUTINE ENTR(EN,ENT,N,RELERR,ABSERR,C)
C
C        NUMERICAL COMPUTATION OF ENTROPY TERMS
C
      DIMENSION C(*),EN(*)
      IND=(2*N+1)**2
C
C        IND GIVES THE NUMBER OF FINITE ELEMENTS IN THE GRID
C
      DO 50 K=1,IND
            L=((K-1)/(2*N+1))-N
            I=K-(L+N)*(2*N+1)-N-1
C
C             I*H AND L*H GIVE THE X AND Y COORDINATES OF THE
C             CENTROID OF THE FINITE ELEMENT, RESPECTIVELY
C
C
C        COMPUTE ENTROPY QUADRANT-BY-QUADRANT
C
C        INITIALIZE ENTROPY
C
            EN(K) = 0.
            ENT = 0.
C
C             ENT IS THE ENTROPY. EN(K) IS THE CONTRIBUTION
C             TO THE ENTROPY FROM THE KTH FINITE ELEMENT
C
```

```
C       FIRST QUADRANT
C
              IF (I.EQ.N.OR.L.EQ.N) GOTO 60
              CALL QUAD(N,I,L,C,K,AN,RELERR,ABSERR,1)
              EN(K) = EN(K)+AN
C
C       SECOND QUADRANT
C
60              IF (I.EQ.-N.OR.L.EQ.N) GOTO 70
              CALL QUAD(N,I,L,C,K,AN,RELERR,ABSERR,2)
              EN(K) = EN(K)+AN
C
C       THIRD QUADRANT
C
70              IF (I.EQ.-N.OR.L.EQ.-N) GOTO 80
              CALL QUAD(N,I,L,C,K,AN,RELERR,ABSERR,3)
              EN(K) = EN(K)+AN
C
C       FOURTH QUADRANT
C
80              IF (I.EQ.N.OR.L.EQ.-N) GOTO 90
              CALL QUAD(N,I,L,C,K,AN,RELERR,ABSERR,4)
              EN(K) = EN(K)+AN
90        ENT = ENT+C(K)*EN(K)
50        CONTINUE
       RETURN
       END
C
C       FUNCTION SUBPROGRAM FOR INTEGRAND
C
       FUNCTION FN(X,J,I,K,N,C,H)
              DIMENSION C(*)
              IF (J.EQ.1.OR.J.EQ.4) GOTO 210
              F=X-(I-1.)*H
              GOTO 220
210              F=(I+1.)*H-X
C
C       THE VALUE OF J WILL DETERMINE WHICH QUADRANT OF THE
C       FINITE ELEMENT WE ARE LOOKING AT.
C
220              IF (J.EQ.1) GOTO 230
              IF (J.EQ.2) GOTO 240
              IF (J.EQ.3) GOTO 250
              GOTO 260
230              AJ = (C(K+N+1)-C(K+1))*(X-I*H)+(C(K+N)-C(K))*((I+1.)*H-X)
              CJ = C(K+1)*(X-I*H)+C(K)*((I+1.)*H-X)
```

```
         GOTO 300
240         AJ = (C(K+N-1)-C(K-1))*(I*H-X)+(C(K+N)-C(K))*(X-(I-1.)*H)
         CJ = C(K-1)*(I*H-X)+C(K)*(X-(I-1.)*H)
         GOTO 300
250         AJ = (C(K-N-1)-C(K-1))*(I*H-X)+(C(K-N)-C(K))*(X-(I-1.)*H)
         CJ = C(K-1)*(I*H-X)+C(K)*(X-(I-1.)*H)
         GOTO 300
260         AJ = (C(K-N+1)-C(K+1))*(X-I*H)+(C(K-N)-C(K))*((I+1.)*H-X)
         CJ = C(K+1)*(X-I*H)+C(K)*((I+1.)*H-X)
300         IF (AJ.EQ.0.) GOTO 310
         IF (ABS(AJ).LT.1E-6) GOTO 310
         BJ=AJ+CJ
         G = BJ*BJ*LOG(BJ)/(2.*AJ*AJ)-CJ*(AJ+BJ)*LOG(CJ)/(2.*AJ*AJ)
     D              -CJ/(2.*AJ)
         GOTO 320
310         G = .75 + .5*LOG(CJ)
320      FN = F * G
      RETURN
      END
C
C
      SUBROUTINE QUAD(N,I,L,C,K,AN,RELERR,ABSERR,J)
C
C      QUAD SETS UP THE PARAMETERS FOR THE NUMERICAL QUADRATURE
C      QUANC8 PERFORMS AN 8-POINT ADAPTIVE GRID QUADRATURE.
C
         DIMENSION C(*)
         H=1./N
         IF (J.EQ.1.OR.J.EQ.4) GOTO 110
         A = (I-1.)*H
         B = I*H
         GOTO 115
110         A = I*H
         B = (I+1.)*H
115      CALL QUANC8(A,B,ABSERR,RELERR,RESULT,ERREST,NOFUN,FLAG,
     D              J,I,K,N,C,H)
      IF (FLAG.NE.0.) WRITE(*,2) FLAG
2      FORMAT (48H WARNING..RESULT MAY BE UNRELIABLE.      FLAG = ,F6.2)
      AN = RESULT+(H*H/4.)*(LOG(4.)-LOG(H))-3.*H*H/8.
      RETURN
      END
```

```
C
C     SUBPROGRAM FOR ADAPTIVE GRID QUADRATURE
C
      SUBROUTINE QUANC8(A,B,ABSERR,RELERR,RESULT,ERREST,NOFUN,FLAG,
     D                       J,I,K,N,C,H)
C
C
      DIMENSION QRIGHT(31),F(16),X(16),FSAVE(8,30),XSAVE(8,30),C(*)
C
      LEVMIN=1
      LEVMAX=30
      LEVOUT=6
      NOMAX=5000
      NOFIN=NOMAX-8*(LEVMAX-LEVOUT+2**(LEVOUT+1))
C
      W0=3956./14175.
      W1=23552./14175.
      W2=-3712./14175.
      W3=41984./14175.
      W4=-18160./14175.
C
C
      FLAG=0.
      RESULT=0.
      COR11=0.
      ERREST=0.
      AREA=0.
      NOFUN=0
      IF (A.EQ.B) RETURN
C
C
      LEV=0
      NIM=1
      X0=A
      X(16)=B
      QPREV=0.
      F0=FN(X0,J,I,K,N,C,H)
      STONE=(B-A)/16.
      X(8)=(X0+X(16))/2.
      X(4)=(X0+X(8))/2.
      X(12)=(X(8)+X(16))/2.
      X(2)=(X0+X(4))/2.
      X(6)=(X(4)+X(8))/2.
      X(10)=(X(8)+X(12))/2.
      X(14)=(X(12)+X(16))/2.
      DO 25 JT=2,16,2
25      F(JT)=FN(X(JT),J,I,K,N,C,H)
      NOFUN=9
C
```

```
C
30      X(1)=(X0+X(2))/2.
      F(1)=FN(X(1),J,I,K,N,C,H)
      DO 35 JP=3,15,2
            X(JP) = (X(JP-1)+X(JP+1))/2.
35          F(JP)=FN(X(JP),J,I,K,N,C,H)
      NOFUN=NOFUN+8
      STEP=(X(16)-X0)/16.
      QLEFT=(W0*(F0+F(8))+W1*(F(1)+F(7))+W2*(F(2)+F(6))
     D       +W3*(F(3)+F(5))+W4*F(4))*STEP
      QRIGHT(LEV+1)=(W0*(F(8)+F(16))+W1*(F(9)+F(15))+W2*(F(10)+F(14))
     D       +W3*(F(11)+F(13))+W4*F(12))*STEP
      QNOW=QLEFT+QRIGHT(LEV+1)
      QDIFF=QNOW-QPREV
      AREA=AREA+QDIFF
C
C
      ESTERR=ABS(QDIFF)/1023.
      TOLERR=AMAX1(ABSERR,RELERR*ABS(AREA))*(STEP/STONE)
      IF (LEV.LT.LEVMIN) GOTO 50
      IF (LEV.GE.LEVMAX) GOTO 62
      IF (NOFUN.GT.NOFIN) GOTO 60
      IF (ESTERR.LE.TOLERR) GOTO 70
C
C
50      NIM=2*NIM
      LEV=LEV+1
C
      DO 52 IT=1,8
            FSAVE(IT,LEV)=F(IT+8)
52          XSAVE(IT,LEV)=X(IT+8)
C
      QPREV=QLEFT
      DO 55 IQ=1,8
            JQ=-IQ
            F(2*JQ+18)=F(JQ+9)
55          X(2*JQ+18)=X(JQ+9)
      GOTO 30
C
60      NOFIN=2*NOFIN
      LEVMAX=LEVOUT
      FLAG=FLAG+(B-X0)/(B-A)
      GOTO 70
C
62      FLAG=FLAG+1.
C
70      RESULT=RESULT+QNOW
      ERREST=ERREST+ESTERR
      COR11=COR11+QDIFF/1023.
C
```

```
C
72       IF (NIM.EQ.2*(NIM/2)) GOTO 75
             NIM=NIM/2
             LEV=LEV-1
             GOTO 72
75       NIM=NIM+1
      IF (LEV.LE.0) GOTO 80
C
      QPREV=QRIGHT(LEV)
      X0=X(16)
      F0=F(16)
      DO 78 IL=1,8
             F(2*IL)=FSAVE(IL,LEV)
78             X(2*IL)=XSAVE(IL,LEV)
      GOTO 30
C
C
80       RESULT=RESULT+COR11
C
C
      IF (ERREST.EQ.0.) RETURN
82       TEMP=ABS(RESULT)+ERREST
      IF (TEMP.NE.ABS(RESULT)) RETURN
      ERREST=2.*ERREST
      GOTO 82
      END
```

DISTRIBUTION LIST

No. of Copies	Organization
12	Administrator Defense Technical Info Center ATTN: DTIC-FDAC Cameron Station, Bldg 5 Alexandria, VA 22304-6145
1	Commander USA Concepts Analysis Agency ATTN: D. Hardison 8120 Woodmont Avenue Bethesda, MD 20014-2797
1	HQDA/DAMA-ZA Washington, DC 20310-2500
1	HQDA, DAMA-CSM, Washington, DC 20310-2500
1	HQDA/SARDA Washington, DC 20310-2500
1	C.I.A. OIR/DB/Standard GE47 HQ Washington, D.C. 20505
6	National Bureau of Standards ATTN: J. Hastie M. Jacox T. Kashiwagi H. Semerjian S. Ray A. Carasso U.S. Department of Commerce Washington, D.C. 20234
1	Commander US Army War College ATTN: Library-FF229 Carlisle Barracks, PA 17013
1	US Army Ballistic Missile Defense Systems Command Advanced Technology Center P. O. Box 1500 Huntsville, AL 35807-3801
1	Chairman DOD Explosives Safety Board Room 856-C Hoffman Bldg. 1 2461 Eisenhower Avenue Alexandria, VA 22331-9999
1	Commander US Army Materiel Command ATTN: AMCPM-GCM-WF 5001 Eisenhower Avenue Alexandria, VA 22333-5001
1	Commander US Army Materiel Command ATTN: AMCDRA-ST 5001 Eisenhower Avenue Alexandria, VA 22333-5001
1	Commander US Army Materiel Command ATTN: AMCDE-DW 5001 Eisenhower Avenue Alexandria, VA 22333-5001
5	Project Manager Cannon Artillery Weapons System, ARDC, AMCCOM ATTN: AMCPM-CW, AMCPM-CWW AMCPM-CWS M. Fisette AMCPM-CWA H. Hassmann AMCPM-CWA-S R. DeKleine Dover, NJ 07801-5001
2	Project Manager Munitions Production Base Modernization and Expansion ATTN: AMCPM-PBM, A. Siklosi AMCPM-PBM-E, L. Laibson Dover, NJ 07801-5001
3	Project Manager Tank Main Armament System ATTN: AMCPM-TMA, K. Russell AMCPM-TMA-105 AMCPM-TMA-120 Dover, NJ 07801-5001
1	Commander US Army Watervliet Arsenal ATTN: SARWV-RD, R. Thierry Watervliet, NY 12189-5001
1	Commander U.S. Army ARDEC ATTN: SMCAR-MSI Dover, NJ 07801-5001
1	Commander U.S. Army ARDEC ATTN: SMCAR-TDC Dover, NJ 07801-5001
4	Commander US Army Armament Munitions and Chemical Command ATTN: AMSMC-IMP-L Rock Island, IL 61299-7300

DISTRIBUTION LIST

No. of Copies	Organization
1	HQDA DAMA-ART-M Washington, DC 20310-2500
1	Commander US Army AMCCOM ARDEC CCAC ATTN: SMCAR-CCB-TL Benet Weapons Laboratory Watervliet, NY 12189-4050
3	Commander US Army ARDEC ATTN: SMCAR-MSI SMCAR-TDC SMCAR-LC LTC N. Barron Dover, NJ 07801-5001
7	Commander US Army ARDEC ATTN: SMCAR-LCA A. Beardell D. Downs S. Einstein S. Westley S. Bernstein C. Roller J. Rutkowski Dover, NJ 07801-5001
3	Commander US Army ARDEC ATTN: SMCAR-LCB-I D. Spring SMCAR-LCE SMCAR-LCM-E S. Kaplowitz Dover, NJ 07801-5001
4	Commander US Army ARDEC ATTN: SMCAR-LCS SMCAR-LCU-CT E. Barrieres R. Davitt SMCAR-LCU-CV C. Mandala Dover, NJ 07801-5001
3	Commander US Army ARDEC ATTN: SMCAR-LCW-A M. Salsbury SMCAR-SCA L. Stiefel B. Brodman Dover, NJ 07801-5001

No. of Copies	Organization
1	Commander US Army Aviation Systems Command ATTN: AMSAV-ES 4300 Goodfellow Blvd. St. Louis, MO 63120-1798
1	Director US Army Aviation Research and Technology Activity Ames Research Center Moffett Field, CA 94035-1099
1	Commander US Army Communications - Electronics Command ATTN: AMSEL-ED Fort Monmouth, NJ 07703-5301
1	Commander CECOM R&D Technical Library ATTN: AMSEL-M-L (Report Section) B.2700 Fort Monmouth, NJ 07703-5000
1	Commander US Army Harry Diamond Lab. ATTN: DELHD-TA-L 2800 Powder Mill Road Adelphi, MD 20783-1145
1	Commander US Army Missile Command ATTN: AMSMI-RX M.W. Thauer Redstone Arsenal, AL 35898-5249
1	Commander US Army Missile and Space Intelligence Center ATTN: AIAMS-YDL Redstone Arsenal, AL 35898-5500
1	Commander US Army Missile Command Research, Development, and Engineering Center ATTN: AMSMI-RD Redstone Arsenal, AL 35898-5245
1	Commandant US Army Aviation School ATTN: Aviation Agency Fort Rucker, AL 36360

DISTRIBUTION LIST

No. of Copies	Organization
1	Commander US Army Tank Automotive Command ATTN: AMSTA-TSL Warren, MI 48397-5000
1	Commander US Army Tank Automotive Command ATTN: AMSTA-CG Warren, MI 48397-5000
1	Project Manager Improved TOW Vehicle ATTN: AMCPM-ITV US Army Tank Automotive Command Warren, MI 48397-5000
2	Program Manager M1 Abrams Tank System ATTN: AMCPM-GMC-SA, T. Dean Warren, MI 48092-2498
1	Project Manager Fighting Vehicle Systems ATTN: AMCPM-FVS Warren, MI 48092-2498
1	President US Army Armor & Engineer Board ATTN: ATZK-AD-S Fort Knox, KY 40121-5200
1	Project Manager M-60 Tank Development ATTN: AMCPM-M60TD Warren, MI 48092-2498
1	Director US Army TRADOC Systems Analysis Activity ATTN: ATOR-TSL White Sands Missile Range, NM 88002
1	Commander US Army Training & Doctrine Command ATTN: ATCD-MA/ MAJ Williams Fort Monroe, VA 23651
2	Commander US Army Materials and Mechanics Research Center ATTN: AMXMR-ATL Tech Library Watertown, MA 02172
1	Commander US Army Research Office ATTN: Tech Library P. O. Box 12211 Research Triangle Park, NC 27709-2211
1	Commander US Army Belvoir Research and Development Center ATTN: STRBE-WC Fort Belvoir, VA 22060-5606
1	Commander US Army Logistics Mgmt Ctr Defense Logistics Studies Fort Lee, VA 23801
1	Commandant US Army Infantry School ATTN: ATSH-CD-CS-OR Fort Benning, GA 31905-5400
1	Commandant US Army Command and General Staff College Fort Leavenworth, KS 66027
1	Commandant US Army Special Warfare School ATTN: Rev & Tng Lit Div Fort Bragg, NC 28307
3	Commander Radford Army Ammunition Plant ATTN: SMCRA-QA/HI LIB Radford, VA 24141-0298
1	Commander US Army Foreign Science & Technology Center ATTN: AMXST-MC-3 220 Seventh Street, NE Charlottesville, VA 22901-5396
2	Commandant US Army Field Artillery Center & School ATTN: ATSF-CO-MW, B. Willis Ft. Sill, OK 73503-5600
1	Commander US Army Development and Employment Agency ATTN: MODE-ORO Fort Lewis, WA 98433-5099

DISTRIBUTION LIST

No. of Copies	Organization
1	Office of Naval Research ATTN: Code 473, R. S. Miller 800 N. Quincy Street Arlington, VA 22217-9999
3	Commandant US Army Armor School ATTN: ATZK-CD-MS M. Falkovitch Armor Agency Fort Knox, KY 40121-5215
2	Commander Naval Sea Systems Command ATTN: SEA 62R SEA 64 Washington, DC 20362-5101
1	Commander Naval Air Systems Command ATTN: AIR-954-Tech Lib Washington, DC 20360
1	Assistant Secretary of the Navy (R, E, and S) ATTN: R. Reichenbach Room 5E787 Pentagon Bldg. Washington, DC 20350
1	Naval Research Lab Tech Library Washington, DC 20375
5	Commander Naval Research Laboratory ATTN: L. Harvey J. McDonald E. Oran J. Shnur R. Doyle Washington, D.C. 20375
5	Commander Naval Surface Weapons Center ATTN: Code G33, J. L. East W. Burrell J. Johndrow Code G23, D. McClure Code DX-21 Tech Lib Dahlgren, VA 22448-5000
2	Comander US Naval Surface Weapons Center ATTN: J. P. Consaga C. Gotzmer Indian Head, MD 20640-5000
4	Commander Naval Surface Weapons Center ATTN: S. Jacobs/Code 240 Code 730 K. Kim/Code R-13 R. Bernecker Silver Spring, MD 20903-5000
2	Commanding Officer Naval Underwater Systems Center Energy Conversion Dept. ATTN: CODE 5B331, R. S. Lazar Tech Lib Newport, RI 02840
4	Commander Naval Weapons Center ATTN: Code 388, R. L. Derr C. F. Price T. Boggs Info. Sci. Div. China Lake, CA 93555-6001
2	Superintendent Naval Postgraduate School Dept. of Mech. Engineering Monterey, CA 93943-5100
1	Program Manager AFOSR Directorate of Aerospace Sciences ATTN: L. H. Caveny Bolling AFB, DC 20332-0001
5	Commander Naval Ordnance Station ATTN: P. L. Stang L Torreyson T. C. Smith D. Brooks Tech Library Indian Head, MD 20640-5000
1	AFSC/SDOA Andrews AFB, MD 20334
3	AFRPL/DY, Stop 24 ATTN: J. Levine/DYCR R. Corley/DYC D. Williams/DYCC Edwards AFB, CA 93523-5000
1	AFRPL/TSTL (Tech Library) Stop 24 Edwards AFB, CA 93523-5000
1	AFATL/DLYV Eglin AFB, FL 32542-5000

DISTRIBUTION LIST

No. of Copies	Organization
1	AFATL/DLXP Eglin AFB, FL 32542-5000
1	AFATL/DLJE Eglin AFB, FL 32542-5000
1	AFATL/DOIL ATTN: (Tech Info Center) Eglin AFB, FL 32542-5438
1	NASA Langley Research Center ATTN: G.B. Northam/MS 168 Langley Station Hampton, CA 23365
1	NASA/Lyndon B. Johnson Space Center ATTN: NHS-22, Library Section Houston, TX 77054
1	AFELM, The Rand Corporation ATTN: Library D (Required or Classified Only) 1700 Main Street Santa Monica CA 90401-3297
1	American Science and Engineers, Inc. ATTN: R. Chase 33-37 Broadway Arlington, VA 02174
2	AAI Corporation ATTN: J. Hebert J. Frankle P. O. Box 6767 Baltimore, MD 21204
1	Aerojet Ordnance Company ATTN: D. Thatcher 2521 Michelle Drive Tustin, CA 92680-7014
1	Aerojet Solid Propulsion Co. ATTN: P. Micheli Sacramento, CA 95813
1	Arnold Engineering Development Center Air Force Department of Technology ATTN: COL L. Keel MS-900 Arnold A.F. Station, TN 37389
1	Arnold Engineering, Development Center Sverdrup Technology, Inc. ATTN: Dr. Ron Belz, MS-930 Arnold A.F. Station, TN 37389
1	Atlantic Research Corporation ATTN: K. King 5390 Cheorokee Avenue Alexandria, VA 22312-2302
1	AVCO Everett Rsch Lab ATTN: D. Stickler 2385 Revere Beach Parkway Everett, MA 02149-5936
1	Bio-Imaging Research, Inc. ATTN: B. G. Isaacson 425 Barclay Blvd Lincolnshire, IL 60029
1	Battelle Memorial Institute ATTN: Tech Library 505 King Avenue Columbus, OH 43201-2693
2	Bell Laboratories ATTN: M. Sondhi F. Shepp Murray Hill, NJ 07971
2	Calspan Corporation ATTN: C. Morphy P. O. Box 400 Buffalo, NY 14225-0400
1	General Electric Company Armament Systems Dept. ATTN: M. J. Bulman, Room 1311 128 Lakeside Avenue Burlington, VT 05401-4985
1	General Electric Computer Research Medical Diagnostics Systems Program ATTN: T. Kincaid Schenectady, NY 12345
1	General Applied Sciences Lab ATTN: J. Erdos Merrick & Stewart Avenues Westbury Long Isld, NY 11590
1	General Motors Rsch Labs Physics Department ATTN: R. Teets Warren, MI 48090

DISTRIBUTION LIST

No. of Copies	Organization
1	IITRI ATTN: M. J. Klein 10 W. 35th Street Chicago, IL 60616-3799
1	Hercules Inc. Allegheny Ballistics Laboratory ATTN: R. B. Miller P. O. Box 210 Cumberland, MD 21501-0210
1	Hercules, Inc. Bacchus Works ATTN: K. P. McCarty P. O. Box 98 Magna, UT 84044-0098
1	Hercules, Inc. Radford Army Ammunition Plant ATTN: J. Pierce Radford, VA 24141-0299
1	Harry Diamond Laboratories ATTN: DELHD-RT-RD P. J. Emmerman 2800 Powder Mill Road Adelphi, MD 20738
3	Hewlett-Packard Corp. ATTN: F. Charbonnier L. Bailey A. Kennedy 1700 South Baker Street McMinnville, OR 97128
1	Honeywell, Inc. - MN64 2200 Defense Systems Division ATTN: C. Hargreaves 6110 Blue Circle Drive Minnetonka MN 55436
1	Institute of Gas Technology ATTN: D. Gidaspow 3424 S. State Street Chicago, IL 60616-3896
1	Lawrence Livermore National Laboratory ATTN: C. Westbrook P.O. Box 808 Livermore, CA 94550
1	Lawrence Livermore National Laboratory ATTN: L-355, A. Buckingham M. Finger P. O. Box 808 Livermore, CA 94550-0622

No. of Copies	Organization
1	Lawrence Livermore National Laboratory ATTN: L-324/M. Constantino P. O. Box 808 Livermore, CA 94550-0622
3	Los Alamos National Lab ATTN: B. Nichols T7, MS-B284 C. Mader K. Hanson P.O. Box 1663 Los Alamos, NM 87545
1	Massachusetts Institute of Technology Laboratory for Information and Decision Systems ATTN: A. S. Wilsky Cambridge, MA 02139-4307
1	Massachusetts Institute of Technology Dept of Mechanical Engineering ATTN: T. Toong 77 Massachetts Avenue Cambridge, MA 02139-4307
2	Mathematics Research Center ATTN: B. Noble J. Nohel 610 Walnut Street Madison, WI 53706
3	Mayo Clinic Biodynamics Research Unit ATTN: E. L. Ritman J. H. Kinsey R. A. Robb 200 First Street, S.W. Rochester, MN 55902
1	Olin Corporation Badger Army Ammunition Plant ATTN: R. J. Thiede Baraboo, WI 53913
1	Olin Corporation Smokeless Powder Operations ATTN: D. C. Mann P.O. Box 222 St. Marks, FL 32355-0222
1	Paul Gough Associates, Inc. ATTN: P. S. Gough P. O. Box 1614, 1048 South St. Portsmouth, NH 03801-1614

DISTRIBUTION LIST

No. of Copies	Organization
1	Physics International Company ATTN: Library H. Wayne Wampler 2700 Merced Street San Leandro, CA 94577-5602
1	Princeton Combustion Research Lab., Inc. ATTN: N.A. Messina 475 US Highway One Monmouth Junction, NJ 08852-9650
2	Rockwell International Rocketdyne Division ATTN: BA08 J. E. Flanagan J. Gray 6633 Canoga Avenue Canoga Park, CA 91303-2703
1	Science Applications, Inc. ATTN: R. B. Edelman 23146 Cumorah Crest Drive Woodland Hills, CA 91364-3710
1	Scientific Research Associates, Inc. ATTN: H. McDonald P.O. Box 498 Glastonbury, CT 06033
3	Thiokol Corporation Huntsville Division ATTN: D. Flanigan R. Glick Tech Library Huntsville, AL 35807
2	Thiokol Corporation Elkton Division ATTN: R. Biddle Tech Lib. P. O. Box 241 Elkton, MD 21921-0241
2	United Technologies Chemical Systems Division ATTN: R. Brown Tech Library P. O. Box 358 Sunnyvale, CA 94086-9998
1	Veritay Technology, Inc. ATTN: E. Fisher 4845 Millersport Hwy. P. O. Box 305 East Amherst, NY 14051-0305

No. of Copies	Organization
1	Universal Propulsion Company ATTN: H. J. McSpadden Black Canyon Stage 1 Box 1140 Phoenix, AZ 85029
1	Battelle Memorial Institute ATTN: Tech Library 505 King Avenue Columbus, OH 43201-2693
1	Brigham Young University Dept. of Chemical Engineering ATTN: M. Beckstead Provo, UT 84601
1	California Institute of Tech 204 Karman Lab Main Stop 301-46 ATTN: F. E. C. Culick 1201 E. California Street Pasadena, CA 91109
1	California Institute of Tech Jet Propulsion Laboratory ATTN: L. D. Strand 4800 Oak Grove Drive Pasadena, CA 91109-8099
1	University of Arizona Optical Sciences Center ATTN: B. Roy Frieden Tucson, AZ 85721
1	University of California, Berkeley Mechanical Engineering Dept. ATTN: J. Daily Berkeley, CA 94720
1	University of California Donner Laboratory ATTN: T.F. Budinger Berkeley, CA 94720
1	University of California, San Diego Energy Center and Dep. Applied Mechanics ATTN: S. S. Penner La Jolla, CA 92037
1	University of Florida Dept. of Chemistry ATTN: J. Winefordner Gainesville, FL 32611

DISTRIBUTION LIST

No. of Copies	Organization
1	University of Illinois Dept of Mech/Indust Engr ATTN: H. Krier 144 MEB; 1206 N. Green St. Urbana, IL 61801-2978
1	University of Illinois Dept of Theoretical & Applied Mechanics ATTN: R. J. Adrian 216 Talbot Lab 104 South Wright St. Urbana, IL 61801
1	University of Massachusetts Dept. of Mech. Engineering ATTN: K. Jakus Amherst, MA 01002-0014
1	University of Michigan Department of Mechanical Engineering ATTN: C. M. Vest Ann Arbor, MI 48104
1	University of Minnesota Dept. of Mech. Engineering ATTN: E. Fletcher Minneapolis, MN 55414-3368
1	University of North Carolina Bio-Medical Engineering Department ATTN: F. A. DiBianca Chapel Hill, NC 27514
1	Oregon State University Department of Mathematics ATTN; K. Smith Corvallis, OR 97133
1	Hospital of the University of Pennsylvania Department of Radiology ATTN: G. T. Herman 3400 Spruce Street Philadelphia, PA 19104
1	Case Western Reserve University Division of Aerospace Sciences ATTN: J. Tien Cleveland, OH 44135
1	George Washington University School of Engineering and Applied Science ATTN: R. Goulard Washington, D.C. 20052

No. of Copies	Organization
3	Georgia Institute of Tech School of Aerospace Eng. ATTN: B. T. Zinn E. Price W. C. Strahle Atlanta, GA 30332
1	Virginia Polytechnic Institute and State University ATTN: J.A. Schetz R. T. Smith Blacksburg, VA 24061
1	Institute of Gas Technology ATTN: D. Gidaspow 3424 S. State Street Chicago, IL 60616-3896
1	Johns Hopkins University Applied Physics Laboratory Chemical Propulsion Information Agency ATTN: T. Christian Johns Hopkins Road Laurel, MD 20707-0690
1	Washington University Mallinckrodt Institute of Radiology ATTN: M. W. Vannier 510 S. Kings Highway St. Louis, MO 63110
1	Massachusetts Institute of Technology Dept of Mechanical Engineering ATTN: T. Toong 77 Massachetts Avenue Cambridge, MA 02139-4307
1	G. M. Faeth Pennsylvania State University Applied Research Laboratory University Park, PA 16802-7501
1	Pennsylvania State University Dept. of Mech. Engineering ATTN: K. Kuo University Park, PA 16802-7501
1	Princeton University MAE Dept. ATTN: F. A. Williams Princeton, NJ 08544

DISTRIBUTION LIST

No. of Copies	Organization
2	Purdue University School of Mechanical Engineering ATTN: N. M. Laurendeau S. N. B. Murthy TSPC Chaffee Hall West Lafayette, IN 47907-1199
1	Purdue University School of Aeronautics and Astronautics ATTN: J. R. Osborn Grissom Hall West Lafayette, IN 47906
1	SRI International Propulsion Sciences Division ATTN: Tech Library 333 Ravenswood Avenue Menlo Park, CA 94025-3493
1	Stanford University Dept. of Mechanical Engineering ATTN: R. Hanson Stanford, CA 94305
1	Stanford University *Department of Physic* ATTN: A. Macovski Palo Alto, CA 94305
1	University of Utah Department of Mathematics ATTN: F. Stenger Salt Lake City, UT 84112
1	Rensselaer Polytechnic Inst. Department of Mathematics Troy, NY 12181
2	Director Los Alamos Scientific Lab ATTN: T3, D. Butler M. Division, B. Craig P. O. Box 1663 Los Alamos, NM 87544
1	Stevens Institute of Technology Davidson Laboratory ATTN: R. McAlevy, III Castle Point Station Hoboken, NJ 07030-5907
1	Rutgers University Dept. of Mechanical and Aerospace Engineering ATTN: S. Temkin University Heights Campus New Brunswick, NJ 08903

No. of Copies	Organization
1	University of Southern California Mechanical Engineering Dept. ATTN: 0HE200, M. Gerstein Los Angeles, CA 90089-5199
2	University of Utah Dept. of Chemical Engineering ATTN: A. Baer G. Flandro Salt Lake City, UT 84112-1194
1	Washington State University Dept. of Mech. Engineering ATTN: C. T. Crowe Pullman, WA 99163-5201

Aberdeen Proving Ground

Dir, USAMSAA
ATTN: AMXSY-D
AMXSY-MP, H. Cohen

Cdr, USATECOM
ATTN: AMSTE-SI-F
AMSTE-CM-F, L. Nealley

Cdr, CSTA
ATTN: STECS-AS-H, R. Hendricksen

Cdr, CRDC, AMCCOM
ATTN: SMCCR-RSP-A
SMCCR-MU
SMCCR-SPS-IL

USER EVALUATION SHEET/CHANGE OF ADDRESS

This Laboratory undertakes a continuing effort to improve the quality of the reports it publishes. Your comments/answers to the items/questions below will aid us in our efforts.

1. BRL Report Number____________________Date of Report__________

2. Date Report Received______________________________

3. Does this report satisfy a need? (Comment on purpose, related project, or other area of interest for which the report will be used.)__________

4. How specifically, is the report being used? (Information source, design data, procedure, source of ideas, etc.)__________

5. Has the information in this report led to any quantitative savings as far as man-hours or dollars saved, operating costs avoided or efficiencies achieved, etc? If so, please elaborate.__________

6. General Comments. What do you think should be changed to improve future reports? (Indicate changes to organization, technical content, format, etc.)

CURRENT ADDRESS

Name

Organization

Address

City, State, Zip

7. If indicating a Change of Address or Address Correction, please provide the New or Correct Address in Block 6 above and the Old or Incorrect address below.

OLD ADDRESS

Name

Organization

Address

City, State, Zip

(Remove this sheet, fold as indicated, staple or tape closed, and mail.)

FOLD HERE

Director
US Army Ballistic Research Laboratory
ATTN: DRXBR-OD-ST
Aberdeen Proving Ground, MD 21005-5066

NO POSTAGE
NECESSARY
IF MAILED
IN THE
UNITED STATES

OFFICIAL BUSINESS
PENALTY FOR PRIVATE USE, $300

BUSINESS REPLY MAIL
FIRST CLASS PERMIT NO 12062 WASHINGTON, DC

POSTAGE WILL BE PAID BY DEPARTMENT OF THE ARMY

Director
US Army Ballistic Research Laboratory
ATTN: DRXBR-OD-ST
Aberdeen Proving Ground, MD 21005-9989

FOLD HERE

END
9-87
DTIC